Corrosion Science xxx (2010) xxx–xxx

Contents lists available at ScienceDirect

Corrosion Science

journal homepage: www.elsevier.com/locate/corsci

The corrosion behaviour of WC-VC-Co hardmetals in acidic media

D.S. Konadu [a], J. van der Merwe [a], J.H. Potgieter [b], S. Vermaak-Potgieter [c], C.N. Machio [d,*]

[a] DST/NRF Centre of Excellence in Strong Materials, School of Chemical and Metallurgical Engineering, University of the Witwatersrand, P.O. Private Bag 3, WITS 2050, South Africa
[b] School of Biology, Chemistry and Health Sciences, Division of Chemistry and Materials, Manchester Metropolitan University, Oxford Road, Manchester M 1 5GD, UK
[c] School of Chemistry, University of the Witwatersrand, P.O. Private Bag 3, WITS 2050, South Africa
[d] Council for Scientific and Industrial Research (CSIR), Materials Science and Manufacturing, P.O. Box 395, PRETORIA 0001, South Africa

ARTICLE INFO

Article history:
Received 20 October 2009
Accepted 25 May 2010
Available online xxxx

Keywords:
WC-Co
WC-VC-Co
Polarization
XRD
Raman spectroscopy
Passivity

ABSTRACT

The effect of increasing vanadium carbide (VC) content on the corrosion behaviour of tungsten carbide – 10 wt% cobalt hardmetals was investigated in 1 M hydrochloric (HCl), and sulphuric (H_2SO_4) acids solutions. Increasing VC content makes the open circuit potential (OCP) in the test solutions more negative than the base alloy. Specimens exhibited pseudo passivation in all the test solutions. Increasing VC led to decreasing corrosion current density. However, the corrosion current densities during chronoamperometric tests were lower for 0 wt% VC. XRD and Raman spectroscopy showed that hydrated WO_3 formed in the surface films of all specimens in hydrochloric acid (HCl), while hydrated vanadyl sulphate also formed for higher VC content specimens in sulphuric acid (H_2SO_4).

1. Introduction

Tungsten carbides or cemented carbides are composite materials consisting of tungsten carbide (WC) grains cemented together by a metallic binder, most commonly cobalt (Co). They are known for their combined high hardness, due to the hard WC phase and working toughness due to the binder. Other carbides are introduced in WC-Co to improve specific properties, e.g., processability, mechanical or corrosion properties. For example, vanadium carbide (VC) is added to prevent WC grain growth during sintering. Also, the addition of VC of grain sizes less than 2 μm in larger quantities of up to 10 wt% has been found to improve hardness without compromising the toughness at a given cobalt content [1].

Cemented carbides have applications spanning most engineering fields. However, application in chemically aggressive environments is less successful because they are susceptible to corrosion [2]. The corrosion properties in acidic and neutral electrolytes are controlled by the corrosion resistance of the Co binder [3,4]. The Co binder gets modified by dissolving tungsten (W) and carbon (C) during the sintering process [5]. Such compositional modification makes it more corrosion resistant. However, the improvement is only minimal [6,7].

One method that has been used to improve the corrosion resistance is the use of corrosion resistant binders, e.g. Ni, Ni-Cr and Ni-Cr-Mo [8,9]. However, such binders can lead to a significant corrosion of the WC grains [10]. The other method has been the addition of other carbide phases. The corrosion resistance is improved by the introduction of chromium carbide [11]. On the other hand, small amounts of TiC and TaC appear to have no influence on corrosion resistance of WC-Co while higher amounts decrease current density [12]. Small amounts of VC also do not appear to influence the corrosion resistance [7]. However, it has been reported [13] that a substitution of WC by 10 wt% VC in WC-Co hardmetals improves corrosion resistance in sulphuric acid. The effect of higher amounts of VC on the corrosion resistance has not been reported before neither has been results from other electrolytes. This paper presents results of an investigation of the effect of increasing VC content on the corrosion properties of WC-Co in sulphuric (H_2SO_4) and hydrochloric (HCl) acids at constant Co weight percent content.

2. Experimental work

2.1. Materials

The nominal compositions, in weight percent, of the samples investigated are given in Table 1. The VC content was varied from 0 to 27 wt%. Specimen 1 with 0 wt% VC is the base alloy against which the other alloys are compared to. The intention was to have specimens of equal weight percent Co but this was not possible. It is however expected that the small variation in Co content will not influence results appreciably. The microstructures of the specimens, obtained using a JEOL JSM 6510 Scanning Electron

* Corresponding author. Tel.: +27 12 841 2870; fax: +27 12 841 3378.
E-mail address: cmachio@csir.co.za (C.N. Machio).

0010-938X/$ - see front matter © 2010 Published by Elsevier Ltd.
doi:10.1016/j.corsci.2010.05.033

Table 1
Nominal compositions of specimens (in wt%).

Sample	WC (%)	VC (%)	Co (%)
1	90	0	10
2	89.6	0.4	10
3	78	10	12
4	62	27	11

Microscope (SEM) operated in the back scatter electron (BSE) mode are given in Fig. 1. Specimens 1 and 2 (hence forth WC-10Co and WC-0.4VC-10Co, respectively) have the well known double phase microstructure of WC (bright phase) and Co (dark phase). The Co appears as small dark regions cementing the carbide grains together. Specimens 3 and 4 (hence forth WC-10VC-12Co and WC-27VC-11Co., respectively) have a triple phase microstructure of WC, Co and (W,V)C. The (W,V)C grains appear to have the same gray level contrast with the Co binder, but are differentiated by their larger, either spherical or irregular shapes. Both types of microstructures are expected [14]. The VC in specimens WC-10VC-12Co and WC-27VC-11Co occurs as the double carbide (W,V)C because WC dissolves in VC [5]. The occurrence of these phases was confirmed by XRD studies (Fig. 6). The introduction of 0.4 wt% VC, as expected [15], led to a refinement of WC grain size (Fig. 1b)

2.2. Corrosion experiments

The electrolytes used in the corrosion experiments were 1 M H_2SO_4 and 1 M HCl, and were prepared from reagent grade chemicals and distilled water. These solutions are not the environments in which the materials investigated are usually applied in. Their use here is, in keeping with other researchers (Cf. Refs. [3,4,6,7]), primarily for comparison purposes. WC-based hardmetals are usually applied in neutral and near-neutral aqueous working environments [8].

Corrosion experiments were performed on metallographically prepared surfaces. Test samples were polished to a 1 μm surface finish using diamond spray and diamond extender (lubricant) after grinding on Struers, Aka-Piatto, of grades 80, 120, 220, 600, and 1200. The samples were attached to insulating copper wires on one face with an aluminium conductive sticker tape. This was followed by cold mounting using epoxy resin and a catalyst in the sample moulds.

Three types of experiments were performed. Immediately upon immersion of the samples in the electrolytes, the open circuit potential (OCP) was monitored for two hours. This was followed by potentiodynamic anodic polarisation measurements. Lastly, in order to investigate whether corrosion products formed on the sample surfaces, chronoamperometric measurements were done for eight hours using a potential selected from the anodic polarisation curve. The anodic polarisation and chronoamperometric tests were carried out on the same surface and in the same test solution. All tests were done at room temperature using electrolytes that were not de-aerated during testing. Before the experiments were started, the reproducibility of corrosion behaviour was determined by running two potentiodynamic anodic polarisation scans.

The anodic polarization tests were carried out in a cell consisting of three electrodes with the test specimen as the working electrode, a graphite rod as the counter electrode (CE) and a silver/silver chloride electrode (SSE) (Saturated KCl) as the reference electrode. The exposed areas of the working electrode were 0.636 cm^2 for WC-10VC and WC-0.4VC-10Co and 0.525 cm^2 and 1.13 cm^2 for WC-10VC-12Co and WC-27VC-11Co specimens. The areas used were determined by the size of the specimens and their values

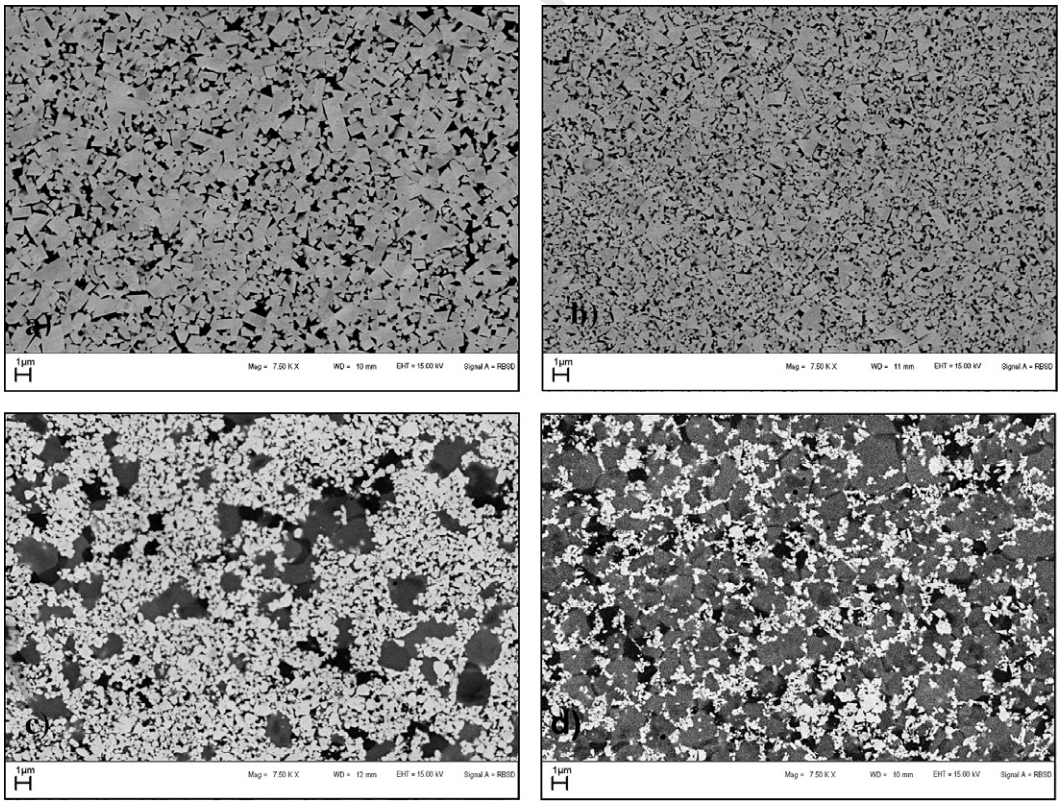

Fig. 1. SEM-BSE microstructures of specimens (a). WC-Co (1), (b). WC-0.4VC-Co (2), (c). WC-10VC-Co (3) and (d). WC-27VC-Co (4) respectively. The light regions in all microstructures are WC while the dark small regions are Co. All the large dark to gray regions in (c and d) are (W, V)C grains.

Please cite this article in press as: D.S. Konadu et al., The corrosion behaviour of WC-VC-Co hardmetals in acidic media, Corros. Sci. (2010), doi:10.1016/j.corsci.2010.05.033

are deemed less important because the per unit area currents were to be quoted. The reference electrode was connected to the cell via a Luggin probe capillary. All the potentials reported were versus the silver-silver chloride standard electrode (SSE) (Saturated KCl). The tests were done using an Autolab potentiostat/galvanostat connected to a personal computer with a General Purpose Electrochemical System (GPES) software. Potential was varied from −600 mV to +1200 mV at a scan rate of 2 mV/s for all the samples. This scan rate is typical of those used in literature even though higher scan rates of 5 mV/s [4] and 50 mV/s [21] have been reported. The scan rate used is not important since the scan rate does not affect the qualitative value of the results [6,21]. The corrosion potential (E_{corr}), and corrosion current density (i_{corr}) for each sample were obtained from the polarization curves according to ASTM standard G5-94. As already stated, all the corrosion experiments were performed after the reproducibility of the potentiodynamic behaviour was determined through repeat runs on repolished test specimens.

Samples were characterized for phases before and after corrosion using a Phillips PW 1710 X-ray diffractometer. Further, after chronoamperometric tests, the samples were cleaned in alcohol and dried and the surfaces analyzed using a Raman microscope spectrometer (Senterra, Bruker Optics) coupled with a Peltier cooled CCD detector. An argon ion laser of wavelength 532 nm was used to generate spectrographs from points on the test surface.

3. Results and discussion

The corrosion behaviour of all the specimens tested was expected to be reproducible because their potentiodynamic anodic polarization scans were reproducible. Fig. 2, obtained from specimen WC-10 VC-12Co, shows the characteristic potentiodynamic polarization behaviour. As a result of this reproducibility of corrosion behaviour, only single scan readings will be provided for all the tests.

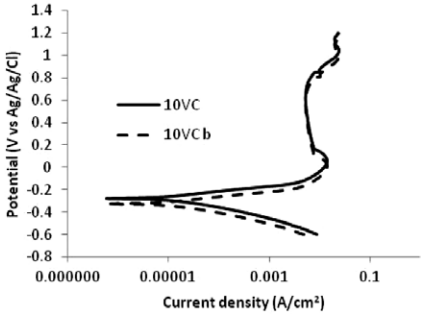

Fig. 2. Potentiodynamic polarisation curves of sample WC-10VC-Co in H_2SO_4 showing excellent reproducibility. Curves 10VC and 10VC b are for the first and second scans respectively.

3.1. Open circuit potential (OCP)

Fig. 3 shows the variation of the OCP of the specimens in HCl and H_2SO_4 solutions. The curves in both solutions are smooth, implying no specimen was susceptible to pitting. The OCP values in HCl decreased within the first hour, implying some corrosion, of maybe a layer of oxide that had formed on the surfaces in air. The OCP values rose slightly on longer immersion, indicating that all the specimens became nobler with time. Increasing VC content made the OCP values in HCl nobler than for the base alloy. However, very high additions made the OCP more negative and specimen WC-27VC-11Co was the least noble. In H_2SO_4, the OCP values were relatively constant throughout the two hours of exposure (Fig. 3b). The introduction of VC produced specimens less noble than the base alloy, with increasing VC shifting OCP values to increasingly more negative values.

3.2. Potentiodynamic polarisation measurements

The potentiodynamic polarisation curves of the samples in HCl are given in Fig. 4a. All the samples exhibited a pseudopassive behaviour marked by a small decrease in the current density at higher potentials. The anodic Tafel constants for the samples with 10VC and 27VC were constant throughout the test. The anodic Tafel constant for the alloy with 0.4VC was highest initially before decreasing to be equal to that of the 10VC and 27VC samples. On the other hand, the anodic Tafel constant for the base alloy was initially equal to that of the 10VC and 27VC samples but suddenly increased at about 0V. This variation of Tafel constant for the base alloy is unlike the case when 1 N HCl is used [6]. The onset of pseudopassive behaviour was earlier for the VC-containing samples, even though the decrease of current density was higher for the base alloy. The pseudo passivation range of the base alloy was small compared to that of the VC-containing samples. The amount of VC did not affect the current density, i_{pass}, in the pseudopassive potential range, and the i_{pass} of the VC samples was higher than for the base alloy.

The potentiodynamic polarisation curves of the samples in H_2SO_4 are given in Fig. 4b. The base alloy WC-10Co and the VC-containing samples all showed pseudo passivation behaviour. The pseudopassivity observed here for the base alloy is in agreement with literature [6,13,17]. The i_{pass} for the VC samples decreased moving from 0.4VC to 10VC. However, further increase in VC did not affect i_{pass}. Unlike in HCl, the anodic Tafel constants for all the samples were very similar in magnitude.

The initial increase of current during anodic polarization in both HCl and H_2SO_4 is attributed to the dissolution of the Co binder, while the increase in current at higher potentials is attributed, for straight WC-Co, to the dissolution of the WC phase [17]. The pseudopassive behaviour observed in both acids is in agreement with literature [6]. The behaviour is termed pseudopassive because the current density decreased only minimally. True passivity oc-

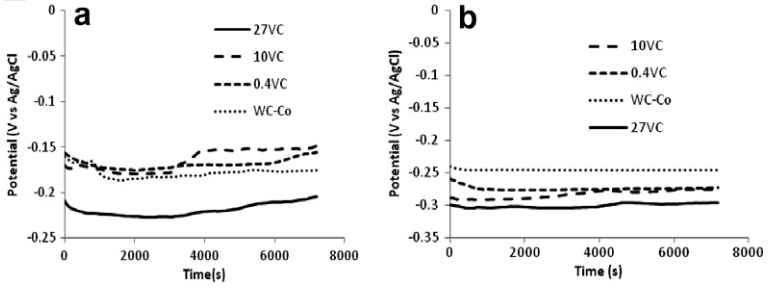

Fig. 3. OCP curves of the WC-VC-Co samples in (a) 1 M HCl and (b) 1 M H_2SO_4.

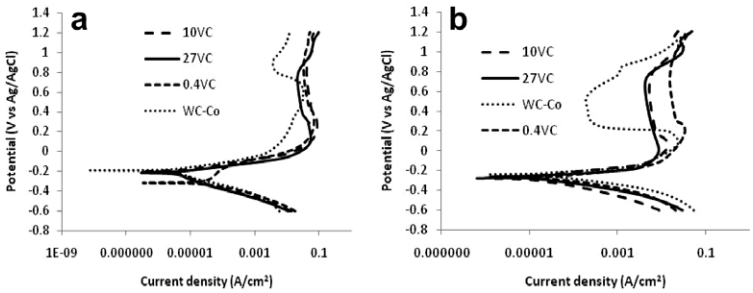

Fig. 4. Potentiodynamic polarisation curves of the samples in (a) HCl and (b) H_2SO_4. Samples exhibit pseudopassive behaviour in both test solutions.

Table 2
The corrosion parameters of the various WC-VC-Co samples in HCl and H_2SO_4.

Sample	HCl		H_2SO_4	
	E_{corr} (V) (SSE)	i_{corr} (μA cm^{-2})	E_{corr} (V) (SSE)	i_{corr} (μA cm^{-2})
WC-10Co	−0.189	1.1	−0.235	5.6
WC-0.4VC-10Co	−0.317	11.0	−0.271	9.3
WC-10VC-12Co	−0.915	1.0	−0.274	4.5
WC-27VC-11Co	−0.213	0.3	−0.263	2.8

curs when the i_{pass} is less than 10 μA cm^{-2} [17]. The pseudo passivation behaviour will be explained in latter sections.

The corrosion parameters of the various WC-VC-Co hardmetals in HCl and H_2SO_4 are given in Table 2. As already noted, these parameters were determined following ASTM Standard G5-94. In this standard, the corrosion current density is determined as the intersection of a line drawn through the corrosion potential, E_{corr}, and a tangent to the linear region of either the cathodic or anodic sections of the polarization curve in the vicinity of E_{corr}. The base alloy, WC-Co, was nobler than the VC-containing alloys in both electrolytes. This observation mirrors that obtained when smaller amounts of VC are involved [11]. The most negative E_{corr} occurred in HCl, for alloy WC-0.4VC-10Co. This might have been caused by the higher anodic Tafel constant for this alloy/electrolyte combination. In H_2SO_4, the E_{corr} values of the specimens were very similar, probably because of the similarity in the anodic Tafel constants. In general, the E_{corr} of the base alloy, WC-Co, in both test solutions is positive to values obtained in literature [4,18]. It is possible that this might have been caused by the difference in the concentrations of electrolytes used. The i_{corr} values in both HCl and H_2SO_4 decreased with increasing VC content. This was caused by the decreasing volume fraction of the binder with increasing VC content. The i_{corr} values are higher in H_2SO_4 than in HCl unlike literature [6]. This observation will be addressed in the sections below.

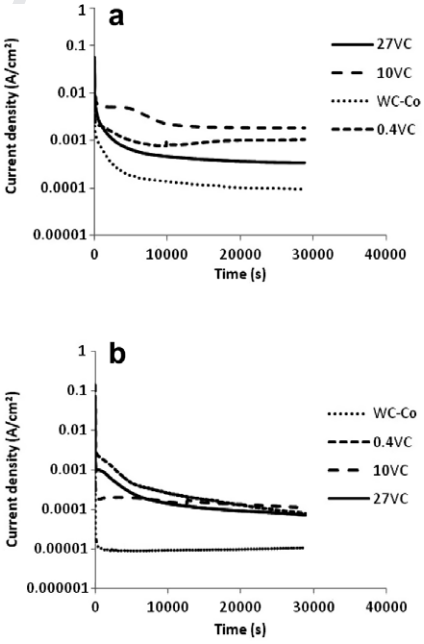

Fig. 5. Variation of current densities during chronoamperometric testing of the various WC-VC-Co samples in (a) HCl and (b) H_2SO_4. Tests in HCl were done at 0.6 V (SSE) for the WC-VC-Co specimens and 0.85 V (SSE) for the base alloy, WC-Co. The potentials used in H_2SO_4 were 0.5 V (SSE) for WC-Co and 0.7 V (SSE) for WC-VC-Co.

3.3. Chronoamperometry

The potentials used for chronoamperometric testing were selected from portions of the anodic polarisation curves where the anodic currents were independent of the applied potential. The potentials used in HCl were 0.6 V (SSE) for the WC-VC-Co hardmetals and 0.85 V (SSE) for the straight WC-Co grade. In H_2SO_4, the potentials used were 0.5 V (SSE) for WC-10Co and 0.7 V (SSE) for the VC hardmetals.

The chronoamperometric behaviour of all the samples was characterized by a decay of current densities to steady state values. The base alloy had the least steady state value in both acids, implying that the introduction of VC was not beneficial. Among the VC alloys, the specimen with 27VC had the least steady state current in HCl while there was no difference in H_2SO_4 (Fig. 5a and b). The decay in current densities and their stabilization to steady state values suggests that the samples developed some passivation characteristics, in line with the observations made for the potentiodynamic polarization behaviour [19].

No attempt is being made to compare the current densities here to those obtained in the pseudopassive region of the potentiodynamic polarization curves. This is because by their nature, the chronoamperometric testing conditions are expected to be near steady state conditions and the relatively thick double layer that is expected to form would slow down charge flow and lead to a lower current density. On the other hand, the potentiodynamic tests are expected to be characterized by a rapidly changing and smaller double layer and hence a lower resistance to charge follow

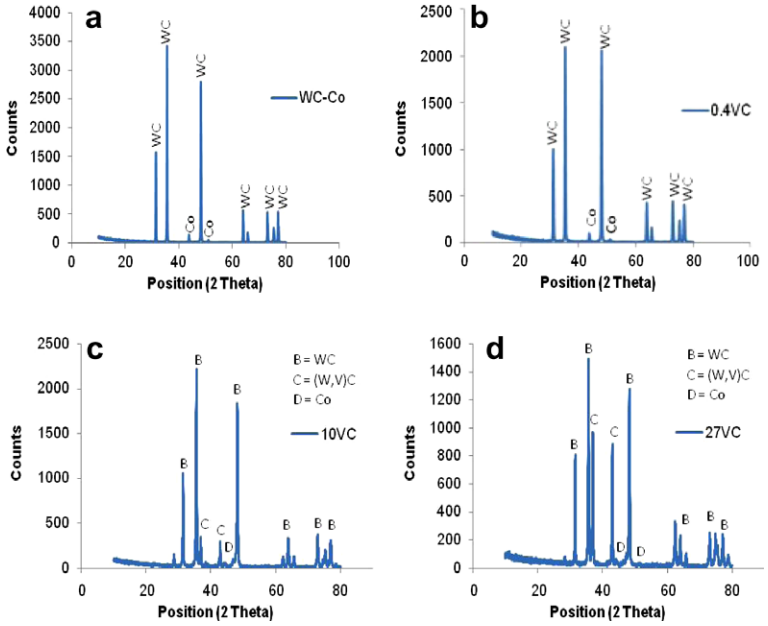

Fig. 6. XRD pattern of WC-VC-Co alloys before corrosion: (a) WC-10Co (b) WC-0.4VC-10Co (c) WC-10VC-12Co (d) WC-27VC-11Co.

that would be accompanied by a higher current density. Similar values of current densities can be obtained only if the scan rates for the potentiostatic and potentiodynamic tests were the same [16].

3.4. Phases before and after corrosion

The XRD patterns of the alloys before corrosion are given in Fig. 6a–d. The phases observed in WC-Co and WC-0.4VC-Co were WC and Co, while (W,V)C also occurred in the 10VC and 27VC samples. No VC peaks were observed in the spectrum of the 0.4VC alloy because the VC content was lower than the detection limit of the XRD. The observation of (W,V)C in the high VC samples here is in agreement with literature [1,13,14,20]. As already mentioned, the (W,V)C forms from the dissolution of WC in VC [5].

Figs. 7a–d and 8a–d show the XRD patterns of the alloys after chronoamperometric tests in HCl and H_2SO_4 respectively. In both acids, all the alloys were missing Co peaks that had appeared before corrosion (Fig. 6a–d), implying that the Co had dissolved in the acids. The dissolution of Co observed here is consistent with literature on the corrosion of WC-based hardmetals [3,4]. The corrosion also led to the formation of new peaks. In HCl (Fig. 7a–d), the new peaks on all the XRD spectra were identified as belonging to hydrated tungsten oxide ($WO_3.H_2O$) for all the samples. In H_2SO_4 (Fig. 8a–d), the new peaks were identified as belonging to hydrated tungsten oxide ($WO_3.xH_2O$, with $x = 1,2$) for WC-10Co and WC-0.4VC-10Co alloys and to hydrated tungsten oxide ($WO_3.H_2O$) and hydrated vanadyl sulphate ($VOSO_4.H_2O$) for the WC-10VC-12Co and WC-27VC-11Co. The formation of the hydrated tungsten oxide in the base alloy is in agreement with literature [21,22].

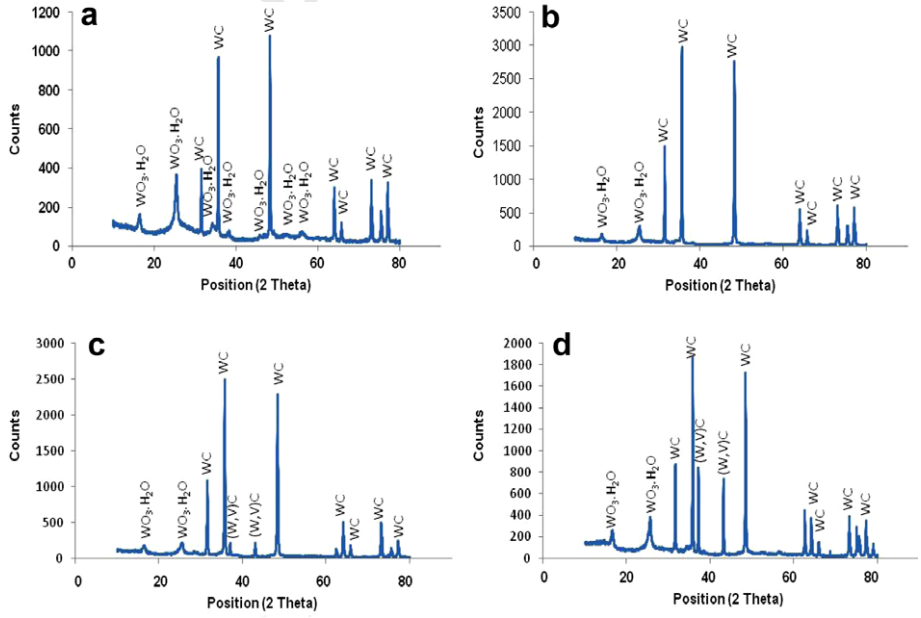

Fig. 7. XRD patterns of sample surfaces after corrosion in HCl: (a) WC-10Co, (b) WC-0.4VC-10Co, (c) WC-10VC-12Co, and (d) WC-27VC-11Co.

Please cite this article in press as: D.S. Konadu et al., The corrosion behaviour of WC-VC-Co hardmetals in acidic media, Corros. Sci. (2010), doi:10.1016/j.corsci.2010.05.033

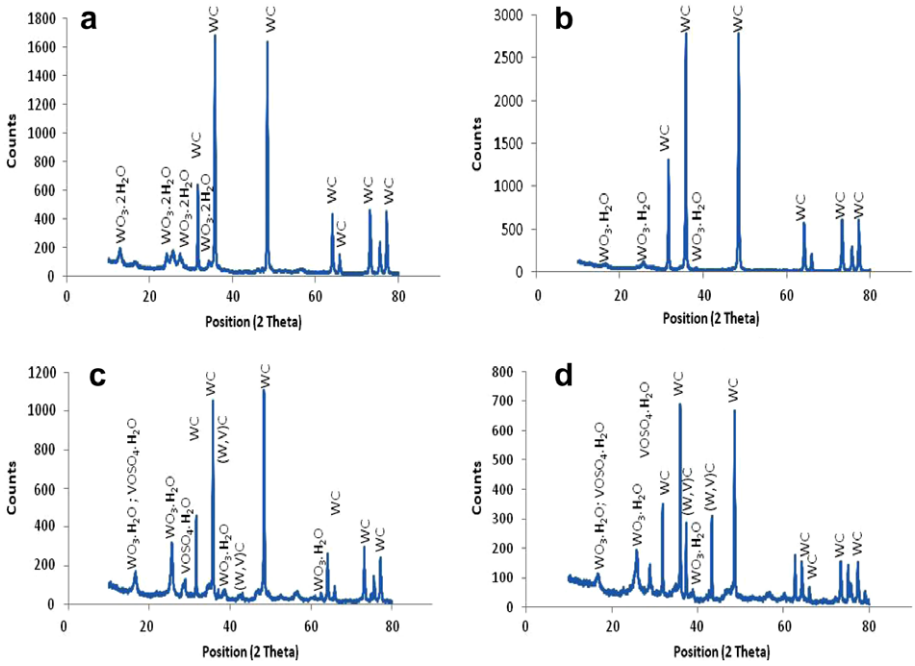

Fig. 8. XRD patterns of the surfaces of the samples after tests in H_2SO_4: (a) WC-10Co, (b) WC-0.4VC-10Co, (c) WC-10VC-12Co, and (d) WC-27VC-11Co.

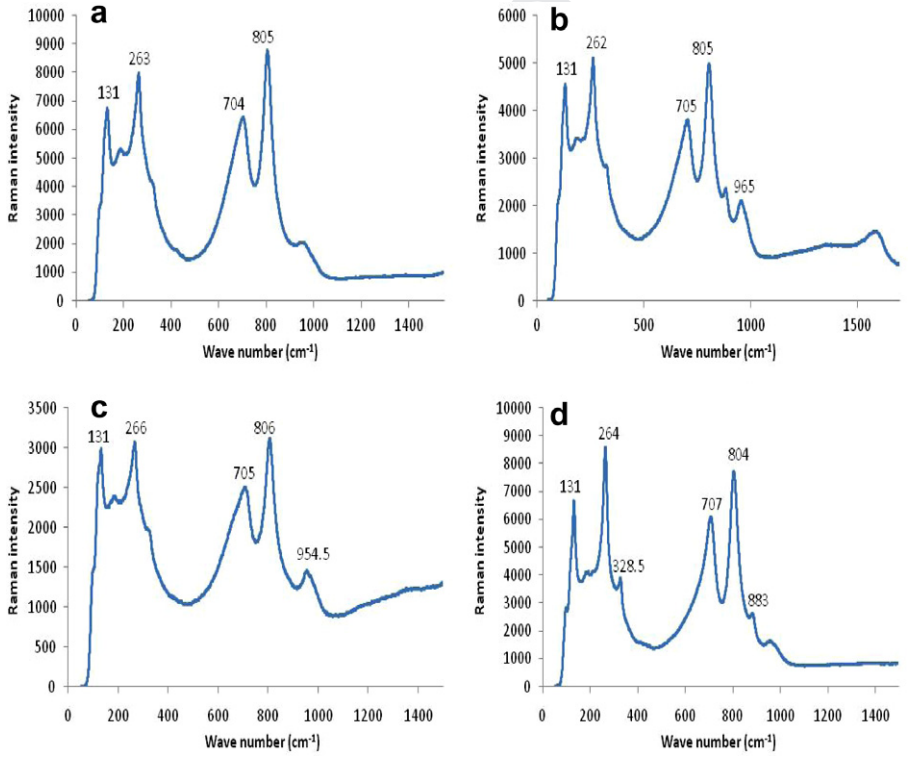

Fig. 9. Raman spectra of corroded product on (a) WC-10Co, (b) WC-0.4VC-10Co, (c) WC-10VC-12Co, and (d) WC-27VC-11Co in HCl.

3.5. Raman spectroscopy

The Raman shifts obtained from the surfaces after chronoamperometric testing in HCl and H_2SO_4 are shown in Figs. 9 and 10 respectively. Several spectrographs were obtained from different points on the same surface and were similar hence only one spectrograph per specimen has been presented here. All the test specimens had, in both acids, Raman bands (Figs. 9a–d and 10a–d) which were attributed to the monoclinic phase of WO_3 and the hydrated tungsten oxide [23–26]. It is known that tungsten oxides form on WC-Co alloys anodically polarized in H_2SO_4 [21,22]. No wave shifts attributable to $VOSO_4.H_2O$ were observed for alloys WC-10VC-12Co and WC-27VC-11Co in H_2SO_4 solution. The observation of tungsten oxides by Raman studies is in agreement with

Please cite this article in press as: D.S. Konadu et al., The corrosion behaviour of WC-VC-Co hardmetals in acidic media, Corros. Sci. (2010), doi:10.1016/j.corsci.2010.05.033

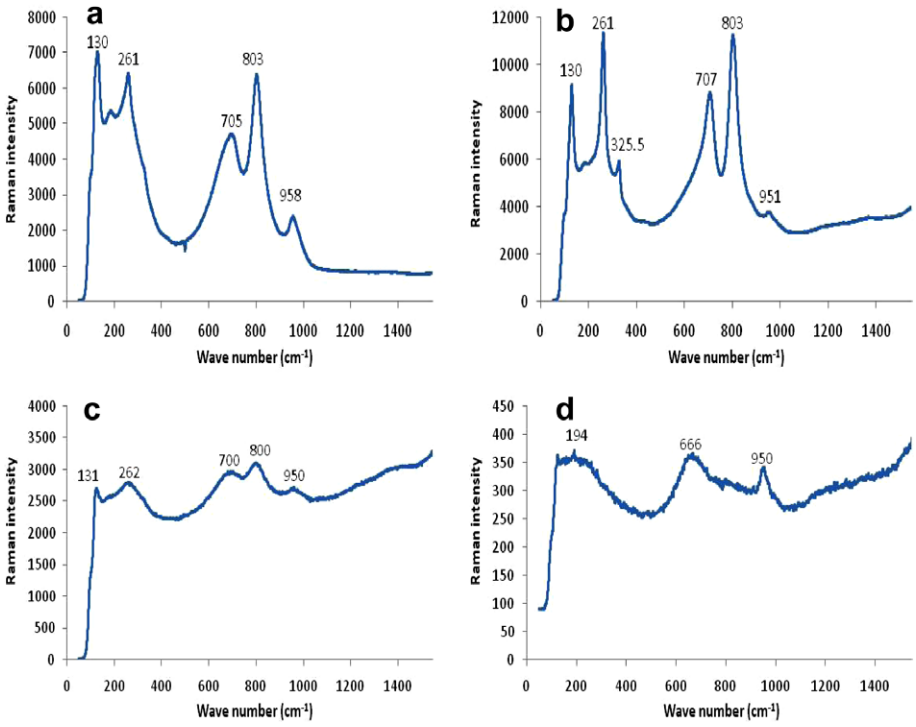

Fig. 10. Raman spectra of corroded product on (a) WC-10Co, (b) WC-0.4VC-10Co, (c) WC-10VC-12Co, and (d) WC-27VC-11Co in H_2SO_4.

the results of XRD analysis of the corroded surfaces (Figs. 7 and 8). No Co based compounds as reported elsewhere in literature [8,9] were observed in the current study after potentiostatic polarization in either HCl or H_2SO_4, probably because, as shown by XRD studies (Figs. 7 and 8) no Co was available.

The observation of the hydrated WO_3 on the surfaces of the samples by both XRD (Figs. 7 and 8) and Raman spectroscopy (Figs. 9 and 10) can help explain the pseudopassivity observed during potentiodynamic polarization (Fig. 4), and also during chronoamperometric tests (Fig. 5). It can be argued that the pseudo passivation could have been caused by the change of composition of the binder during sintering. Under normal circumstances, pure Co is not passivating. During sintering, W and C go into solution in the Co [5] and the presence of W confers pseudo passivation behaviour to the binder [7]. However, the passivation of the binder cannot explain the observed passivation of the composite WC-Co and WC-VC-Co samples. This is because the XRD patterns of all the specimens after corrosion (Figs. 7 and 8) showed that the entire surface Co binder had dissolved.

No VC-based compound was obtained in the surface film of the VC alloys after corrosion in HCl (Figs. 7 and 9). This suggests that VC did not take part in the passivation behaviour of the VC alloys when in HCl. In H_2SO_4, XRD patterns of VC alloys had peaks for $VOSO_4.H_2O$ (Fig. 8) implying that the VC took part in corrosion. This however does not appear to have been beneficial, as was seen from the higher corrosion current densities (Table 2). There were no peaks of $VOSO_4.H_2O$ on the Raman patterns for the VC alloys and it is probable that the compound is not Raman active.

4. Conclusion

The electrochemical corrosion behaviour of WC-VC-Co alloys has been investigated with the help of XRD and Raman spectroscopy. The OCP result showed that the samples were not susceptible to pitting corrosion in both 1 M HCl and H_2SO_4. The introduction of VC in WC-Co improved the passivation resistance of the hardmetals in HCl, and at high VC contents resulted in lower corrosion current densities than for the base alloy in both HCl and H_2SO_4. All the samples showed pseudopassive behaviour in both HCl and H_2SO_4 due to the formation of a passive film of hydrated WO_3 No VC-based corrosion products were observed after corrosion in HCl. In H_2SO_4, the compound $VOSO_4.H_2O$ formed in alloys with high VC contents. However, the formation of $VOSO_4.H_2O$ appears to have been detrimental to corrosion resistance since the corrosion current densities recorded in H_2SO_4 where higher than those recorded in HCl.

Acknowledgement

The authors are grateful to DST's Centre of Excellence in Strong Materials (COE-SM) and National Research Foundation (NRF), South Africa for their financial support.

References

[1] B.S. Luyckx, C. Osborne, L.A. Cornish, D. Whitefield, Powder Metallurgy 39 (3) (1996) 210–212.
[2] H. Engqvist, U. Beste, N. Axén, International Journal of Refractory Metals and Hard Materials 18 (2-3) (2000) 103–109.
[3] M.H. Ghandehari, Journal Electrochemical Society 127 (10) (1980) 2144–2147.
[4] S. Hochstrasser-Kurz, Y. Mueller, C. Latkoczy, S. Virtanen, P. Schmutz, Corrosion Science 49 (4) (2007) 2002–2020.
[5] H.E. Exner, International Metals Reviews 24 (4) (1979) 149–173.
[6] S. Sutthiruangwong, G. Mori, International Journal of Refractory Metals and Hard Materials 21 (3-4) (2003) 135–145.
[7] A.M. Human, B. Roebuck, H.E. Exner, Materials Science and Engineering A241 (1998) 202–210.
[8] B. Bozzini, G.P. De Gaudenzi, M. Serra, A. Fanigliulo, F. Bogani, Materials and Corrosion 53 (5) (2002) 328–334.
[9] H. Scholl, B. Hofman, BA Rauscher, Electrochimica Acta 37 (3) (1992) 447.
[10] M.A. Human, T.I. Northdrop, B.S. Luyckx, N.M. James, Journal of Hard Materials 2 (3–4) (1991) 247–257.
[11] W.J. Tomlison, N.J. Ayerst, J. Materials Science 24 (1989) 2348–2354.
[12] G. Mori, H. Zitter, A. Lackner, M. Schretter, 15th International Plansee Seminar 2 (2001) 222–236.
[13] S.P. Broccardo, M.Sc dissertation, University of the Witwatersrand, Johannesburg (2003).
[14] S. Luyckx, D. Markoulides, I.T. Northrop, D.J. Whitefield, International Journal of Materials and Product Technology 15 (3/4/5) (2000) 270–274.
[15] Geoffrey E Spriggs, International Journal of Refractory Metals & Hard Materials 13 (1995) 241–255.

Please cite this article in press as: D.S. Konadu et al., The corrosion behaviour of WC-VC-Co hardmetals in acidic media, Corros. Sci. (2010), doi:10.1016/j.corsci.2010.05.033

[16] ASTM G5-94: Standard reference test method for making potentiodynamic anodic polarization measurements, ASTM book of standards – 1994.
[17] A.M. Human, H.E. Exner, International Journal of Refractory Metals & Hard Materials 15 (1997) 65–71.
[18] A.M. Human, H.E. Exner, Materials Science and Engineering A 209 (1996) 180–191.
[19] A. Lekatou, E. Regoutas, A.E. Karantzalis, Corrosion Science 50 (12) (2008) 3389–3400.
[20] S. Luyckx, D. J. Whitefield, M. J. Witcomb, and L. A. Cornish, in Advances in powder metallurgy and particulate materials James J Oakes, John H Reinshagen, (Eds.) 1 (1998) 1-85 – 1-91.
[21] B. Bozzini, G.P. De Gaudenzi, A. Fanigliulo, C. Mele, Materials and Corrosion 54 (5) (2003(a)) 295–303.
[22] B. Bozzini, P.D. De Gaudenzi, A. Fanigliulo, C. Mele, Corrosion Science 46 (2) (2004) 453–469.
[23] B. Ingham, S.V. Chong, J.L. Tallon, Journal of Physical Chemistry B 109 (11) (2005) 4936–4940.
[24] M. Regragui, M. Addou, A. Outzourhit, J.C. Bernéde, E. El Idrissi, E. Benseddik, A. Kachouane, Thin Solid Films 358 (1-2) (2000) 40–45.
[25] M.F. Daniel, B. Desbat, J.C. Lassegues, B. Gerand, M. Figlarz, Journal of Solid State Chemistry 67 (2) (1987) 235–247.
[26] M. Gotic, M. Ivanda, S. Popovic, S. Music, Materials Science and Engineering B B77 (2000) 193–201.

Please cite this article in press as: D.S. Konadu et al., The corrosion behaviour of WC-VC-Co hardmetals in acidic media, Corros. Sci. (2010), doi:10.1016/j.corsci.2010.05.033